

# A CRYOGENICALLY COOLED HIGH VOLTAGE DC PHOTOGUN\*

Hyeri Lee<sup>†</sup>, Luca Cultrera, Ivan Bazarov, CLASSE, Ithaca, NY 14853, USA

## Abstract

Linear electron accelerators and their applications such as ultrafast electron diffraction require compact high-brightness electron sources with high voltage and electric field at the photocathode to maximize the electron emission and minimize space-charge induced emittance growth. Achieving high brightness from a compact source is very challenging because this results in an interplay between photoemission, electron acceleration, beam dynamics and HV technology. We present a new design of a compact electron DC high voltage (HV) gun with a novel cryogenic photocathode system and report on construction and commissioning processes. This photogun aims to operate at  $\sim 200$  kV at room temperature (RT) and cryogenic temperature (low T) with a corresponding electric field of 10 MV/m. It hosts a photocathode plug compatible with that used in several other labs, opening the possibility of generating and characterizing electron beam from photocathodes developed at other institutions. This result represents a milestone for compact electron photoemission guns aimed at high brightness electron beam production and applications that benefit from increased brightness.

## INTRODUCTION

Bright electron sources and their applications have become a critical area in electron accelerators: Ultrafast Electron Diffraction (UED), for example, benefits from the bright electrons to observe atomic level dynamics in tabletop setups and a single-shot UED demands shorter bunch lengths and longer coherence lengths at the sample location [1, 2]. Electron beams for protein samples require large transverse coherence  $L_{c,x} \gtrsim 1$  nm, sufficient bunch charges  $q \gtrsim 10^5$  electrons, and short pulse lengths  $\sigma_t \sim 100$  fs [3, 4], confining electrons in a small 6D phase space volume. Multi-alkali antimonide photocathodes provide high brightness electron beams that can meet all of these requirements [5–7].

The transverse coherence length  $L_{c,x}$  for UED becomes a function of electric field  $E_0$  at the cathode and the charge  $q$  at the charge saturation limit for a pancake shape bunch;

$$\frac{L_{c,x}}{\lambda_e} \propto f_\epsilon \sigma_x \sqrt{\frac{m_e c^2}{\text{MTE}}} (E_0/q)^{1/2} \quad (1)$$

depending on the degree of emittance preservation  $f_\epsilon \in (0, 1]$ ,  $\sigma_x$  is the rms laser spot size,  $m_e c^2$  is the electron mass, MTE is the mean transverse energy of the photoelectrons related to the intrinsic emittance  $\epsilon_{i,x} = \sigma_{x,\text{laser}} \sqrt{\text{MTE}/m_e c^2}$  and  $\lambda_e = \hbar/m_e c = 3.862 \dots \times 10^{-4}$  nm is the reduced Compton wavelength of the electron [8, 9]. Note that we need to

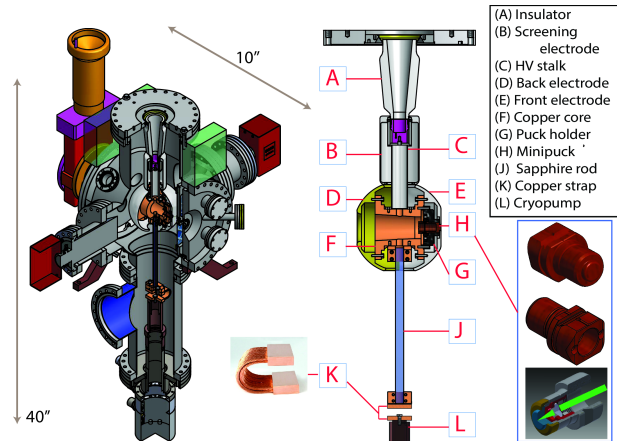


Figure 1: Left: A 3D model of the gun. Right: The internal structure of the gun. Inset: (H) The detailed view of the minipuck and the modified puck with a glass substrate and a focusing lens for transmission mode (bottom). The green arrow indicates a laser focused on the substrate.

maximize  $E_0$  and  $f_\epsilon$  and minimize MTE to obtain longer  $L_{c,x}$ . The emittance can be both minimized and better preserved ( $f_\epsilon \approx 1$ ) by increasing the applied voltage at the cathode [10] at a given cathode-anode gap.

Our recent studies have demonstrated that the intrinsic emittance near the emission threshold decreases from  $0.27 \mu\text{m}/\text{mm}$  (or MTE of  $38 \pm 2$  meV) at 300K to  $0.2 \mu\text{m}/\text{mm}$  (or  $22 \pm 1$  meV) at 90K [5, 6]. This points out a venue for obtaining the smaller photocathode MTEs by cooling down the photocathode substrate to the low temperatures. Recently, our simulations have shown that a photogun with the initial MTE of 5 meV can generate electron beams of  $L_{c,x} \gtrsim 30$  nm at the sample location with  $\sigma_t \approx 100$  fs when focused to the radius  $R = 200 \mu\text{m}$  [8].

In this paper, we present the design of a compact electron photoemission source with a novel cooling scheme built at Cornell University. We describe its mechanical design along with HV performance and thermal measurements. Additionally we demonstrate the first beam from this cryogenically cooled photogun.

## MECHANICAL DESIGN

A schematic view of the gun is shown in Fig. 1. The top half of the gun provides HV and the bottom half cools down the photocathode holding structure to a cryogenic temperature. The top half consists of a main chamber and its side flanges. All parts are made of 304 stainless steel (SST) unless otherwise noted. The inverted insulator was welded to a 10 in. vacuum flange which was installed from the top of the chamber. The anode electrode is a grounded

\* This work has been funded by the National Science Foundation (Grant No. PHY-1416318)

<sup>†</sup> HL823@cornell.edu

flat mesh, 20 mm away from the cathode surface and placed parallel to the flat surface of the spherical electrode.

The inverted insulator (Fig. 1a) is a conical-shaped ceramic ( $Al_2O_3$ ), whose vacuum-side surface is doped with a vendor-proprietary coating for a low-level bulk conductivity. The receptacle side of the insulator fits a HV cable (type R28), which is specified by the length and angle of the receptacle. An HV stalk (Fig. 1c) is attached downward to provide the mechanical support and the electrical connection. A banana connector is installed on the bottom of the receptacle to electrically connect the cable to the HV stalk and the electrodes.

Two electrodes are used in this gun: a screening electrode and a spherical shell electrode. The screening electrode (Fig. 1b) is an SST thin tube shielding the triple point junction, where the insulator, the HV stalk and vacuum meet. The thin tube efficiently reduces the thermal conduction from the insulator to the cryogenic electrode. A spherical shell electrode consists of two hemispheres, made of 316 SST vacuum remelt. The internal electrode structure consists of two oxygen-free high thermal conductivity (OFHC) copper pieces, where the copper core (Fig. 1f) connects the HV stalk to the cryogenic system and the puck holder (Fig. 1g), which holds a photocathode plug in place inside the spherical electrode towards its front.

The bottom half of the gun is a part of the cryogenic system cooling down the electrode with the photocathode and consists of the bottom chamber of the gun and a cold source. The cold source is a cryocooler, widely used for low-temperature systems. The in-vacuum connection between the cryocooler and the copper core is through a sapphire rod (Fig. 1j) and an OFHC flexible strap (Fig. 1k). In order to minimize the temperature rise from the cryocooler to the cathode, the copper and sapphire are used because of their high thermal conductivities. The sapphire rod, in particular, is known for its superb thermal conductivity at cryogenic temperatures as well as its excellent dielectric properties. Two copper pieces clamp the rod at each end connecting the rod to the internal electrode structure and the copper strap. More details of the gun are described elsewhere [11].

### THERMAL MEASUREMENT AND HV CONDITIONING

The thermal profile, a critical part of this gun design, is shown in Fig. 2. Thermal sensors were attached from the internal electrode structure to the cryocooler, with the exact locations and measurements shown in Fig. 2c. The final temperature of the photocathode is  $43 \pm 1$  K after 29 hours of cooling. The uncertainty mainly comes from changes in the external radiation from the ambient temperature surfaces. From the top of the sapphire rod to the bottom of the puck holder, the temperature changes from 29 K to 35 K and then to 43 K at the photocathode.

The gun was installed with a modified 325 kV high-voltage power supply (HVPS) originally from Glassman High Voltage, Inc. The HVPS is located in a custom-made

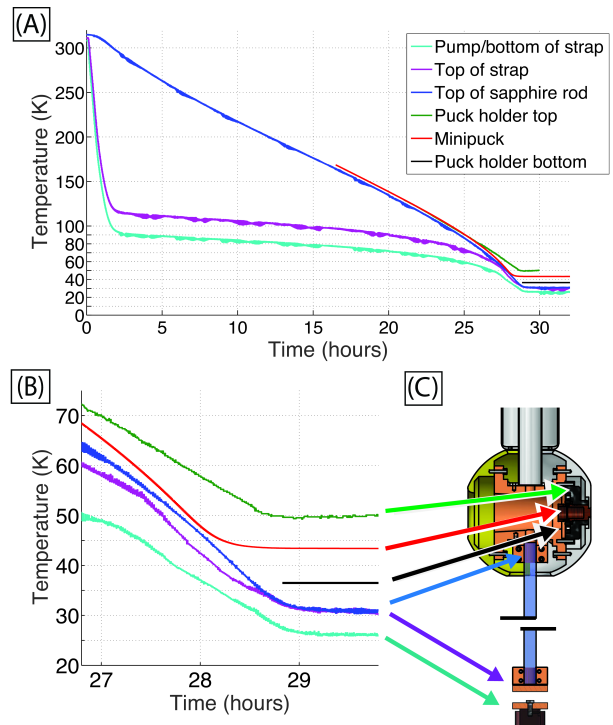


Figure 2: (A) The temperature profile while cool-down of the gun. (B) The profile near the equilibrium. (C) The exact location of the thermal sensors.

chamber and is surrounded by 15 psi sulfur hexafluoride ( $SF_6$ ) as a dielectric to minimize arcing in the HVPS by absorbing free electrons [12]. The HVPS is connected to the gun via an HV cable and a processing resistor chain. The X-ray HV cable is rated up to 270 kV by the manufacturer, Dielectric Sciences, Inc. The processing resistor chain consists of forty nine 4 M $\Omega$  resistors, giving a total resistance of 196 M $\Omega$ . This prevents the gun from damage by excessive currents during an arc [13, 14]. The gun vacuum level is approximately  $2 \times 10^{-11}$  Torr when not HV conditioning.

The goal of the voltage processing is to minimize the field emission at the operating voltage. The field emission extracts unwanted electrons resulting in excessive currents in the gun and followed by radiation and vacuum activities [14, 15]. In order to monitor the processing progress, the currents and the radiation levels are recorded. The floating ammeter reads the current from a processing resistor chain to the gun. A net excess current is defined by the difference between the current read from the ammeter and the current drawn by the insulator.

The processing was performed at room temperature (RT) and then cooled down for further conditioning. The voltage applied to the gun was carefully increased while observing currents and radiation activities. The voltage was increased to  $\sim 150$  kV within the first couple of hours, however, field emitters began to slow down the conditioning process (shown in blue in Fig. 3). The high purity helium gas was introduced via a leak valve to the gun for helium gas processing. The vacuum was increased above  $10^{-5}$  torr with

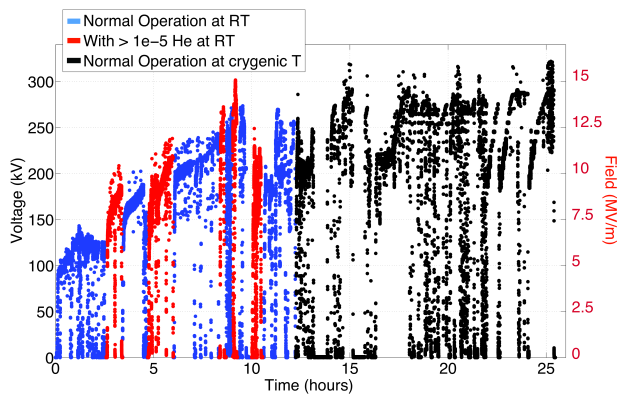


Figure 3: The voltage applied to the gun during the HV processing. The electric field corresponding to the voltage is also shown in red.

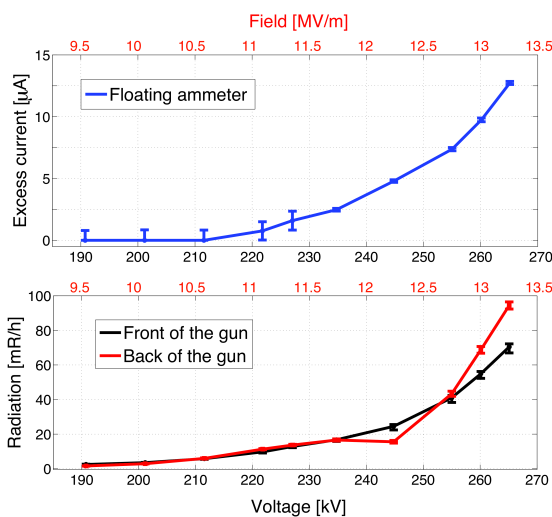


Figure 4: Gun performance data (cryogenic temperature) at the different voltages (black label on x-axis) and the associated electric fields (red). Top: Excess current data. Bottom: Radiation at the front and back of the gun.

ion pumps off. The helium gas processing allowed the persistent emitters to be burn out, achieving a higher voltage of  $\sim 180$  kV as shown in red in Fig. 3. Conditioning continued at RT for 11 hours in total with gas processing and achieved  $\sim 270$  kV maximum.

As soon as the gun cooled down to 43 K at the cathode, the voltage reached above 200 kV without any issue as shown in black in Fig. 3. The goal of processing at the cryogenic temperature is to stabilize the gun at the desired operational voltage of 225 kV [8]. With the continued processing the voltage reached almost 300 kV; however, the processing progress dramatically slowed down compared to the progress at RT. As the electric field beyond 10 MV/m was applied, new emitters opened frequently as soon as old ones were removed. This pattern is seen as ups and downs in Fig. 3.

Finally, the gun became stable near 225 kV. Figure 4 shows the excess current and radiation as a function of applied

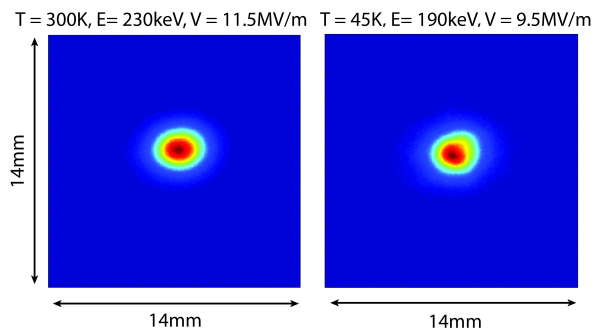


Figure 5: The electron beams generated at RT (left) and cryogenic temperature (right).

voltage and electric field. The first electron beams from  $\text{Cs}_3\text{Sb}$  were imaged on a BeO fluorescent viewscreen  $\sim 37$  cm away from the cathode, shown in Fig. 5.

## CONCLUSION

In summary, we have successfully built a HV DC photoemission gun that allows cooling of photocathode down to cryogenic temperatures. This electron source has several important features: (i) the gun was specifically designed to minimize the emittance (via the photocathode substrate temperature) and maximize the voltage and electric field at the photocathode at the same time; (ii) the physical size and the beam quality of this gun are especially suitable for UED applications as demonstrated by detailed beam dynamics simulations [8]. Finally, we have successfully generated first beam from the photocathode at both RT and the cryogenic temperature. We believe that this gun will have a direct impact for bright electron sources development and their applications.

## REFERENCES

- [1] M. Gao *et al.*, Nature 496, 343 (2013)
- [2] H. Ihee *et al.*, Science 291, 458 (2001)
- [3] German Sciaini and R J Dwayne Miller, Reports on Progress in Physics 74 (2011)
- [4] R. D. Miller, Ann. Rev. Phys. Chem. 65, 583 (2014)
- [5] H. Lee *et al.*, Rev. Sci. Instrum. 86.073309 (2015)
- [6] L. Cultrera *et al.*, Phys. Rev. ST Accel. Beams 18, 113401 (2015)
- [7] J. Maxson *et al.*, Appl. Phys. Lett. 106, 234102 (2015)
- [8] C. Gulliford *et al.*, Phys. Rev. Accel. Beams 19, 093402 (2016)
- [9] I. V. Bazarov, B. M. Dunham, and C. K. Sinclair, Phys. Rev. Lett. 102, 104801 (2009)
- [10] B. J. Siwick *et al.*, J. Appl. Phys. 92, 1643 (2002)
- [11] H. Lee, For brighter electron sources: a cryogenically cooled photocathode and DC photogun, Ph.D. thesis, Cornell University (2017)
- [12] R. Arora and W. Mosch, High voltage and electrical insulation engineering (J. Wiley and Sons, Hoboken, N.J., 2011)

- [13] N. Nishimori *et al.*, in Proceedings of ERL09, Ithaca, NY, USA, Injectors, Guns, and Cathodes (2009) pp. 4–23.
- [14] J. Maxson *et al.*, Rev. Sci. Instrum.85,093306 (2014)
- [15] G. R. Werner, Probing and Modeling Voltage Breakdown in Vacuum, Ph.D. thesis, Cornell University (2014)